Journal of the Serbian Society for Computational Mechanics / Vol. 17 / No. 2, 2023 / pp 55-68
(10.24874/jsscm.2023.17.02.05)

NUMERICAL ANALYSIS OF COMPOUND PARABOLIC SOLAR COLLECTOR WITH TWO GLASS COVERS

Mohammad Omidpanah[1] and Seyyed Abdolreza Gandjalikhan Nassab[2*]

[1] Department of Mechanical Engineering, Technical and Vocational University, Tehran, Iran
e-mail: momidpanah@tvu.ac.ir
[2] Department of Mechanical Engineering, Shahid Bahonar University of Kerman, Kerman, Iran
e-mail: ganj110@uk.ac.ir
**corresponding author*

Abstract

In a compound parabolic solar collector, a glass cover is normally used for decreasing the rate of heat loss from the absorber. In this paper, a solar collector with two glass covers and a concentration ratio of 1.6 is simulated and examined for the purpose of higher performance. The distance between covers is 45 mm and the cavity of solar collector is filled with air. Due to the temperature gradient, the turbulent free convection airflow takes place inside the cavity. As the main aim, the effect of the second glass sheet on performance improvement is examined. Towards this end, the equations govern to the turbulent buoyant airflow in the collector's cavity was numerically solved by the finite element method using the COMSOL Multiphysics software. Also the conduction equation is employed for temperature computation in the solid elements. Numerical findings demonstrate the effective role of the second glass sheet in decreasing the rate of heat loss from solar collectors and a more than 6% increase in the thermal efficiency of the studied test cases is found because of the second glass sheet. Comparison between the numerical findings of free convection airflow with experimental data shows good consistency.

Keywords: compound parabolic collector, turbulent flow, two glazed, efficiency

1. Introduction

In many industrial processes including drying and cooking, desalination, steam generation, and space heating, a heat source in the range of 350-450 K is required. For providing this temperature range, the compound parabolic concentrators (CPCs) with medium concentration ratio may be employed even without using a tracking system (Ari 1975). These types of solar collectors have a relatively wide acceptance angle and operate efficiently during a sunny day with low maintenance costs (Macro et al. 2014 and Macro et al. 2015).

One of an important part of a solar heating system is the absorber by which, the absorbed radiative solar heat flux is transferred to the working fluid. The most common types of collectors are flat plate and tubular collectors. The flat plate collector which is concerned in the present study is the most widely used solar thermal system for several applications. These types of collectors absorb both diffuse and collimated radiations, and therefore still function when beam radiation is cut off by a cloud.

There are much research works on improving the performance of CPCs by several investigators. A large branch of these studies focused on the shape of absorbers. The importance and effect of collector geometry in the design and application of CPCs were verified by Ochieng (2009). A literature review about CPCs with tubular absorbers was reported by Jiang et al. (2020). The design of CPCs with a glass-evacuated glass tube as a solar receiver was obtained as a result of the mentioned studies (Mill et al. 1896, Mill et al. 1994 and Buttinger et al. 2010). A novel parabolic trough solar collecting system with a V-shaped absorber was studied Bie et al. (2020) with the uses of an appropriate mathematical model. The obtained numerical findings have been validated with experiment at different operating conditions. One of the main phenomena which have a great influence on the thermal performance of CPCs is the air-free convection flow inside the cavity of the collector which leads to heat loss from the heated absorber to the ambient from the glass cover. The simulation of buoyant airflow has been highly regarded by many researchers due to its main role in the thermal behavior of solar collectors. As an early work, the natural convection laminar airflow in a CPC cavity was numerically simulated by Chew et al. (1989) and the finite element method (FEM) was employed in simulations. Results were presented for representing these collectors with tubular absorbers of concentration ratio 2. Higher thermal efficiencies were found for CPCs with shallower cavities, especially at large Grashof numbers. The interaction of free convection and surface radiation in CPCs was studied numerically by Diaz et al. (2008). In that study, the finite difference technique was developed to solve the free convection airflow equations. An analytic transformation function was used to map the parabolic shape in the physical domain into a rectangular region as the computational domain. The numerical results showed that the temperature pattern is much affected by the surface radiation inside the solar system. Some correlations for natural convection in CPCs' cavities were determined by Singh et al. (2012) from experimental measurements. The effects of several important factors such as tilting of the solar collectors, truncation of the reflector side walls, and the temperature of inlet water as heat removal fluid have been studied. From the obtained numerical finding, a correlation was derived for prediction of heat loss by natural convection from the heated absorber for a special range of working fluid inlet temperatures. In a great number of published papers, the convection airflow inside the CPC's cavity was studied by CFD methods and the effects of some geometrical parameters and also the value of incoming solar heat flux were examined (Eames et al. 1993 and Antonelli et al. 2016). In a recent study by the author, a novel design of the CPC cavity for decreasing the rate of heat loss was examined by installation of a partial glass sheet in the lower part of the collector (Gandjalikhan Nassab 2022). By this suggested method, the high temperature zone adjacent to the heated absorber is separated from the main convection recirculated airflow and a lower rate of heat loss takes place in the collector. For simulation of thermal system, the flow equations were solved by the CFD technique, and the effect of glass sheets with different lengths on the performance of solar collector was examined. Numerical findings showed a more than 20% efficiency increase for the studied test cases.

A literature review showed that no study has so far been conducted on a numerical study of two glazed CPCs with flat plate absorbers. The novelty of the present research is not only innovates the said issue but may also provide useful guidelines in the design of efficient CPC solar collectors by applying a second glass cover. For this, a CFD-based numerical simulation was performed for analysis of air free convection flow inside the cavity of a full solar collector by numerical solution of the flow equations with FEM. Finally, the effect of second glass cover on the efficiency of solar collector operating under steady condition was explored.

2. Theory

2.1 Governing equations

The schematic of the studied full CPC is presented in Fig. 1. The main elements in this type of solar collectors are the glass cover(s), refractory side walls, absorber plate and the collector cavity in which free convection airflow takes place because of the buoyancy effect. For thermo hydrodynamic simulation of solar collector, the following governing equations for steady Newtonian incompressible turbulent free convective airflow consist of conservation of mass, momentum and energy were solved in this study. The well known standard $\mathrm{k}-\varepsilon$ method was employed for modeling the turbulent nature of airflow closed the RANS problem.

$$\frac{D\rho}{Dt} + \rho\nabla.V = 0 \tag{1}$$

$$\frac{D(\rho V)}{Dt} = -\nabla P + \nabla.[(\mu + \mu_t)(\nabla V + \nabla V^T)] + (\rho - \rho_o)g \tag{2}$$

$$\frac{D(\rho C_p T)}{Dt} = \nabla.\left[\left(k_{th} + \frac{\mu_t}{Pr_t}\right)\nabla T\right] \tag{3}$$

$$\frac{D(\rho k)}{Dt} = \nabla.\left(\left(\mu + \frac{\mu_t}{\sigma_k}\right)\nabla k\right) + P_k + P_b - \rho\epsilon + S_k \tag{4}$$

$$\frac{D(\rho \epsilon)}{Dt} = \nabla.\left(\left(\mu + \frac{\mu_t}{\sigma_\epsilon}\right)\nabla \epsilon\right) + C_1\frac{\epsilon}{k}(P_k + C_3 P_b) - C_2\rho\frac{\epsilon^2}{k} + S_\epsilon \tag{5}$$

Where κ and ϵ are the turbulent kinetic energy and its dissipation rate, $\mu_t = C_\mu \frac{\rho k^2}{\epsilon}$ is the turbulent viscosity, C_1, C_2, C_3 are constants, and P_k, P_b denote turbulent production and buoyancy production, respectively. More details about the governing equation were provided by Gandjalikhan Nassab (2022). Both single glass and double glass CPCs are analyzed in this work, such that the studied solar collectors are exactly similar to each other, while a second glass sheet by a distance of 5 cm is installed below the top cover. The values of some geometrical parameters and thermo-physical properties of solar collectors are reported in Table. 1. In addition, the height of CPC is 55 cm, and the lengths of aperture and absorber are 55 cm and 26 cm, respectively. The Grashof number defined as $Gr = g\beta\Delta TH^3/\nu\alpha$ becomes in the order of 10^9 corresponds to turbulent flow condition (Diaz et al. 2008). The two thin side walls with parabolic shape have refractory surfaces without any absorption and emission.

2.2 Numerical model and solution method

In numerical simulation, a discretized computational domain as illustrated in Fig. 2, was generated with employing appropriate refinements near critical regions, to simulate the boundary layer flow ($y^+ \leq 1$) as reported by Reichl et al. (2013). To obtain the grid independent solution, a mesh study was performed by considering two-dimensional unstructured meshes with 5380 to 12600 elements. In the mesh study, the values of maximum temperature of solar collector as a sensitive parameter to the grid size was computed with a different number of elements and the optimum discretized domain with 10500 grids was distinguished according to Table 2.

All calculations were performed using the COMSOL Multi-physics computer code based on the FEM. The physical model includes surface radiation, conduction and free convective heat transfers. The transmitted solar radiation from the glass cover(s), was completely absorbed by the receiver black top surface, and the bottom surface of this element is in convection heat transfer with the working fluid. The buoyancy forces according to the Bossinesque approximation were computed in flow simulation. The radiation heat transfer inside the cavity of the collector was

computed based on the surface-to-surface radiation model. The studied CPC was assumed to be made of copper for the receiver and glass for the cover, while the two side walls are completely reflectors. The working gas in the cavity i.e. air was modeled as an incompressible ideal gas, whose thermo-physical properties are considered temperature dependent.

Since, the convection boundary condition is applied on the absorber lower surface where this element is in heat transfer with the working fluid, the values of temperature and convection coefficient were imposed by the user. In this regard, the fixed convection coefficient of 50 W/m^2K and working fluid temperature of 350 K were used in simulations. To apply the convection boundary condition for the side walls and the top glass, equivalent convection coefficients including the convection and radiation parts are considered. All of the applied boundary conditions are given in Table. 3.

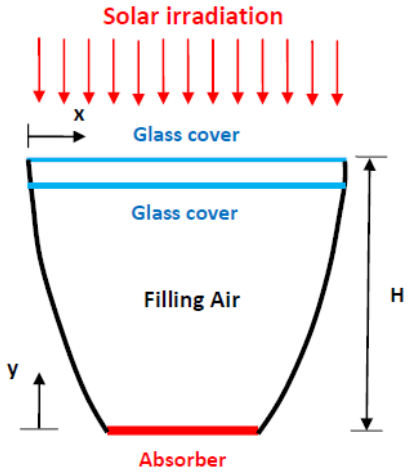

Fig. 1. A schematic of a CPC solar collector with two glass covers.

Physical properties	Top glass cover	Absorber
Length [m]	0.55	0.26
Thickness[mm]	4	10
Thermal conductivity [W/m.K]	0.78	400
Surface emissivity	0.9	0.98
Reflectivity	0.05	0.02
Transmissivity	0.9	0

Table 1. The values parameters used in simulation.

No. of elements	[K]T_{max}	Variation respect to previous step
5380	360.1	-
6720	378.6	4.9%
8400	398.1	1.7%
10500(Opt.)	402.1	1%
12600	402.9	0.2%

Table. 2. Mesh study.

Location	Condition
Top (Absorber)	Constant heat flux, No-slip
Top (Glass cover)	Convection with h_{eq}
Bottom (Absorber)	Convection with working fluid flow
Side walls	Convection with h_{eq}
Air-solid interfaces	Continuity of temperature and heat flux, No-slip

Table 3. Applied boundary conditions.

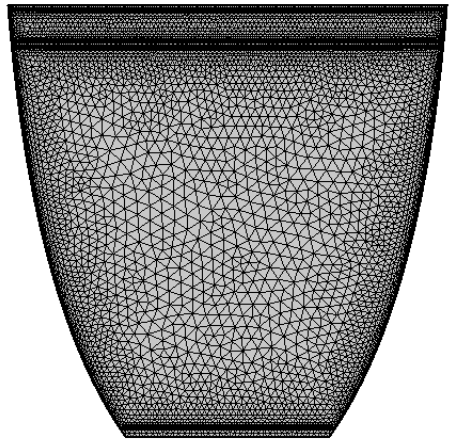

Fig. 2. The discretized computational domain with unstructured triangular grids.

2.3 Validation of numerical results

The result of the present numerical analysis about the computation of free convection flow inside the CPC's cavity was compared with the experimental data found by Cheesewrigth et al. (1986). In that research work, the free convection of airflow in a tall enclosure was studied. The velocity variation at the mid-plane of the cavity is plotted in Fig. 3-a. As seen, the air velocity in the central zone of the cavity is very small and high-velocity air flow near the side walls occurs due to the air density gradient. As seen, Fig. 3-a demonstrates a good agreement between the current numerical study and experimental results. For further validation, the obtained numerical findings are also compares with experimental data given by Singh et al. (2012). In that reference, a detailed experimental work was performed for analysis of the free convective heat transfer in CPC cavities and many correlations about the average Nusselt number on the absorber surface were determined. Experimental findings were reported for CPCs with full-, three quarter- and half-height reflectors, *CR* = 2 and a 100 mm wide flat plate absorber. The two test cases including the full and three quarter CPC were simulated in the present work with the same condition as considered by Singh et al. (2012) and the variations of mean Nusselt number on the absorber surface against the Rayleigh number are plotted and compared with experiment in Fig. 3-b. This figure shows the increasing trend of convection coefficient with Ra for both full and ¾ height CPCs. The consistency between the theoretical results with experiment shows the accuracy of the applied mathematical model and numerical procedure.

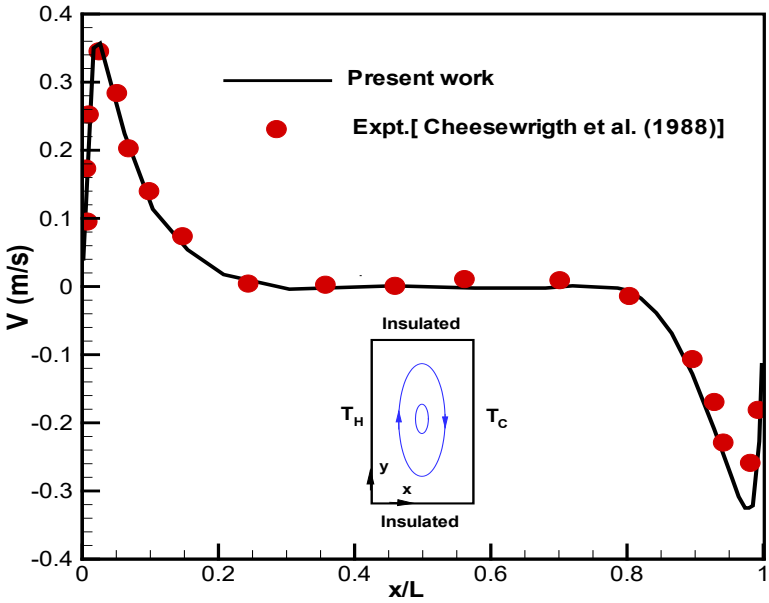

a) Distribution of air velocity along the center-line of enclosure

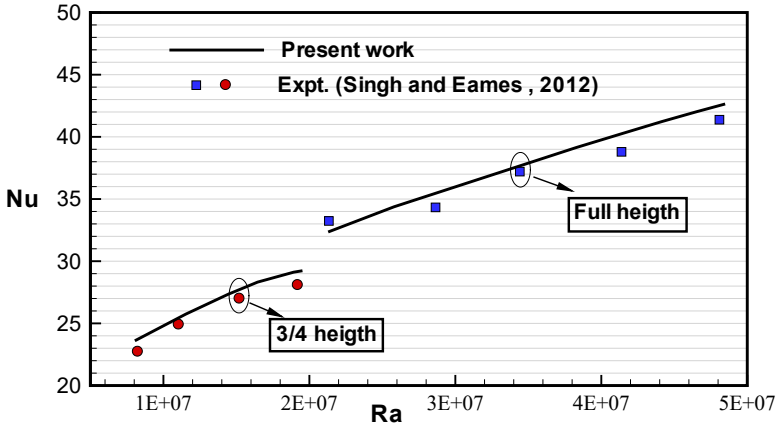

b) Variation of Nusselt number on the heated absorber with Ra

Fig. 3. Comparison of the obtained numerical findings with experiments.

3. Results

The numerical findings of the present study for double-glass CPC solar collector are presented and also compared with a single glass one in this section. In the computations of all subsequent figures, the value of solar heat flux is 900 W/m^2, and the distance between the two covers is kept at 45 mm and the values of other geometrical parameters of solar collector is reported in Table 1.

Representative flow pattern plots for double and single-glazed solar collectors are shown in Figs. 4 and 5, respectively. Inside the thermal collector immediately after initialization from the conduction mode, the free convective airflow always has two recirculated cells lying symmetrically about the centerline of the cavity, as seen in Fig. 4. It should be mentioned that,

whether or not this flow pattern persists depends on several factors such as the Rayleigh number and geometrical parameters. As seen in a solar collector with a single glass cover, the airflow changes from a bicellular to a unicellular pattern because the cavity becomes taller. This finding is in agreement with the numerical results reported in a paper by Abdel-Khalik et al. (1978). Comparison between the velocity magnitude contours in Fig. 4 and 5 demonstrate the effect of the second glass cover in decreasing the airflow velocity. This fact has a positive influence on decreasing the energy loss from the heated absorber and improving the collector performance.

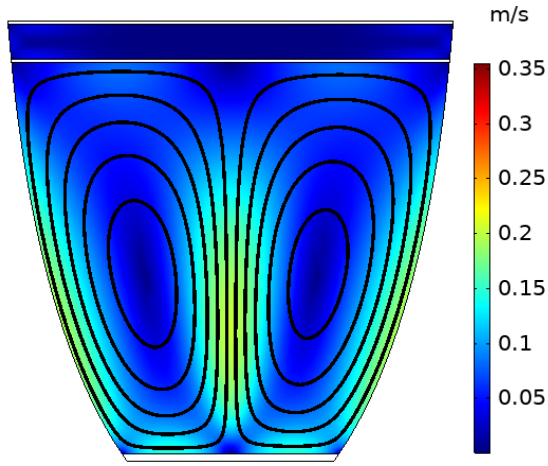

Fig. 4. Velocity magnitude contour in double glass cover CPC.

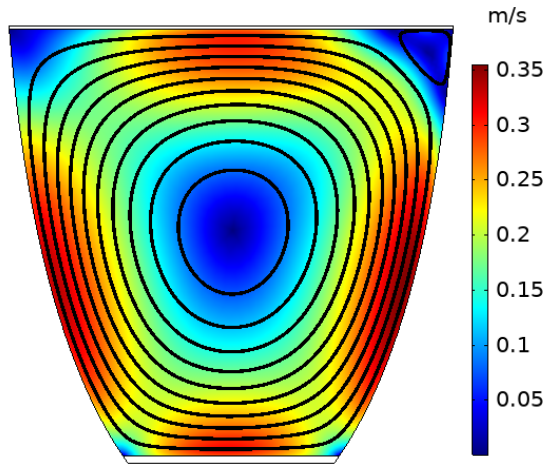

Fig. 5. Velocity magnitude contour in single glass cover CPC.

In Fig. 6, a clear image of the velocity field inside the gap between two glass covers is provided. As seen, a very low velocity inside the convective airflow takes place due to the short height of the air gap and the dominance of boundary surfaces in damping the buoyancy effect. An almost stagnant zone is seen in the central region, such that the air velocity increases near the two ends.

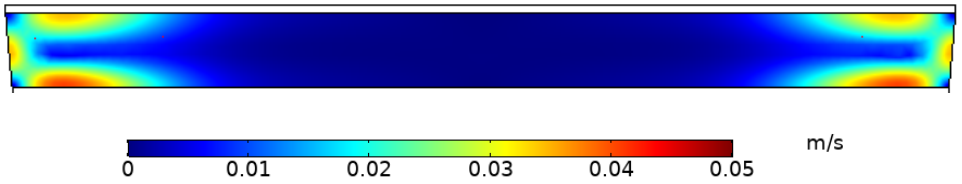

Fig. 6. Velocity magnitude contour inside the gap between the covers.

The vector plots of air velocity fields inside the cavities of the two types of solar collectors are drawn in Fig. 7. The variations of velocity vectors inside the bicellular and unicellular zones in the analyzed solar collectors are clearly seen in this figure, respectively. It should be mentioned that due to the turbulent regime of convection airflow and large velocity gradient inside the boundary layer, the buoyant airflow has almost high velocity near the boundaries.

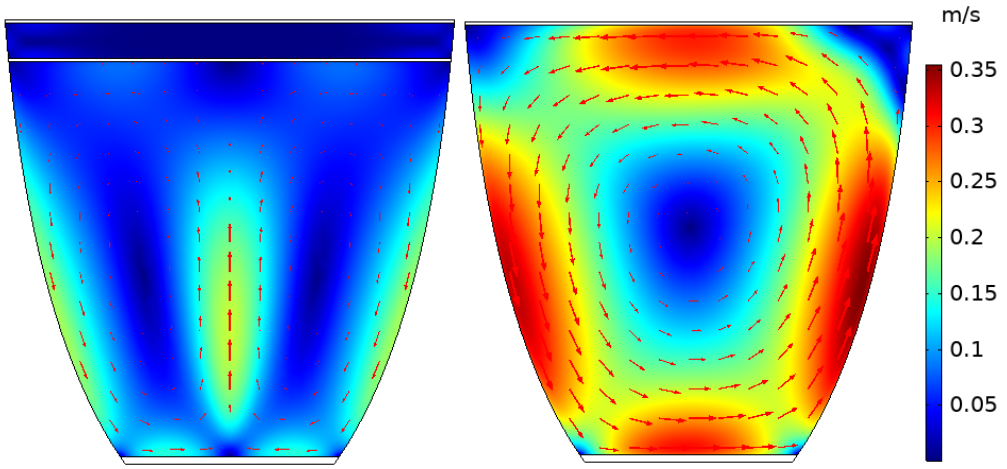

a) Double glass b) Single glass

Fig. 7. Velocity vector field.

The pressure fields for the two test cases are depicted in Fig. 8 by plotting the pressure contours inside the cavities of solar collectors. The high-pressure region closed to the absorber plate is seen in this figure due to the buoyancy effect such that the air pressure decreases along the axes of collectors. Also, it is seen that the presence of second glass does not have a considerable influence on the air convection pressure field.

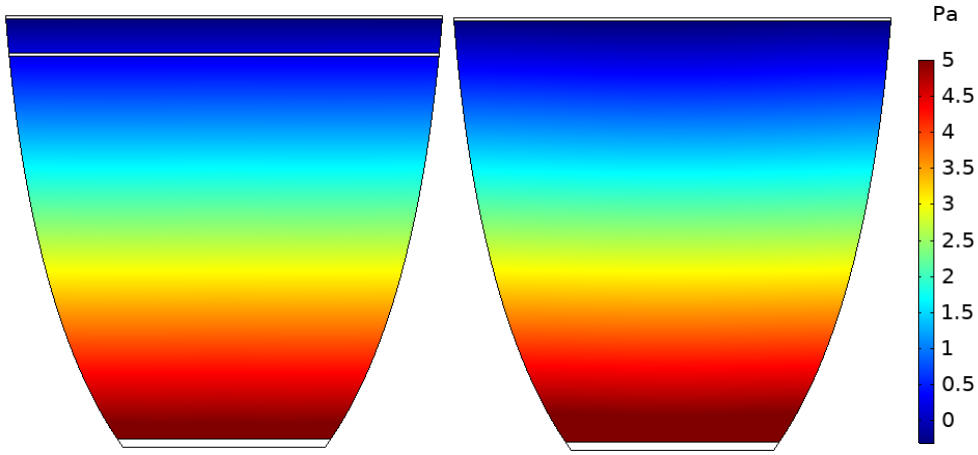

Fig. 8. Pressure contour plot.

The turbulent kinetic energy contours are drawn in Fig. 9. A symmetric field is seen inside the cavity of CPC with two glass covers, such that a small region with high turbulent kinetic energy exists adjacent to the middle of absorber plate where the two recirculated zones reach each other. Fig. 9 shows a higher value for the maximum kinetic energy in the single glass collector, but its pattern is quite different from that found in the two glazed CPC due to different patterns of velocity fields in these thermal systems.

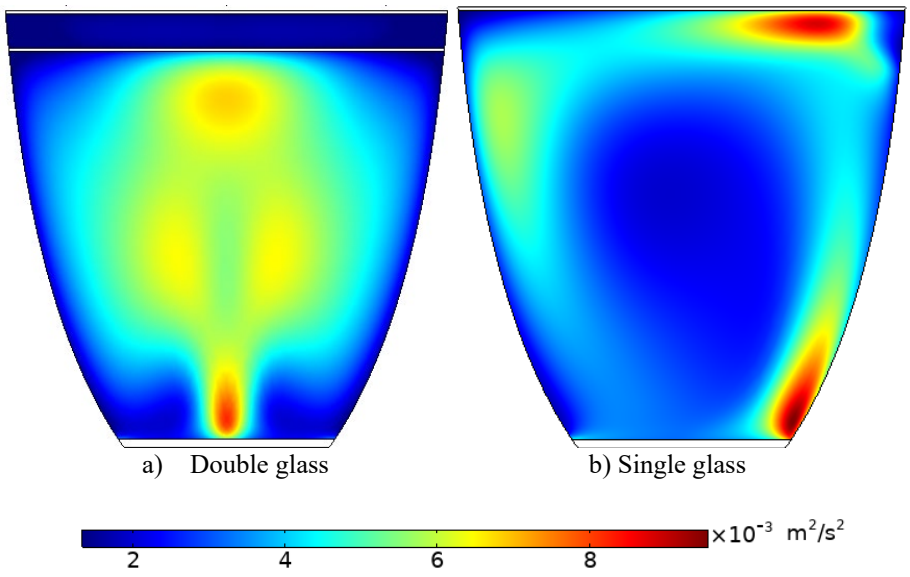

Fig. 9. Contours of turbulent kinetic energy.

To demonstrate the thermal behavior of single and double-glazed CPCs, the temperature contour plots are provided in Fig. 10. A considerable difference is seen between the studied two cases, such that the presence of a second glass sheet causes higher temperature for the absorber

and the air layer closed to this element. This is due to a lowering in energy loss from the collector by the installation of the second glass sheet that leads to the relatively cold region adjacent to the upper glass cover where the main energy loss takes place.

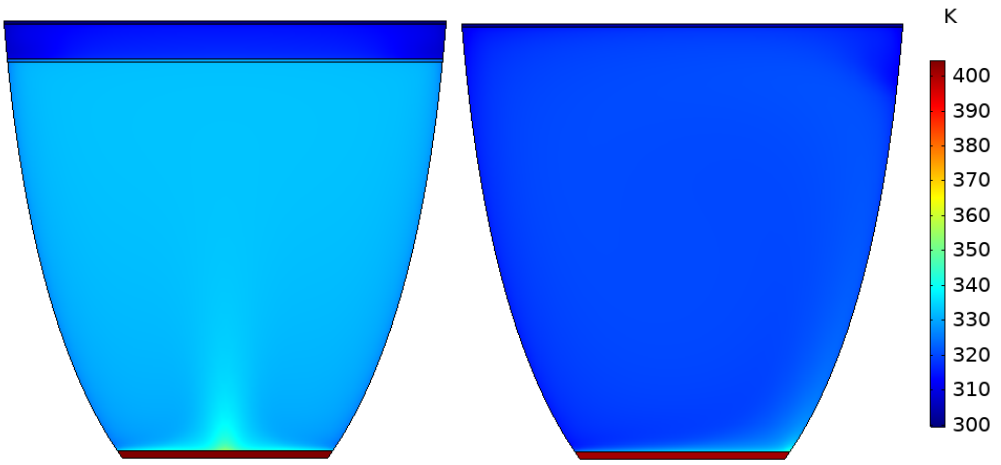

Fig. 10. Temperature field inside the CPC.

For more study about the effect of second glass sheet on the performance of solar collector, the temperature distributions along the upper glass covers for the two test cases are drawn in Fig. 11. For each case, the temperature increases along the glass cover up to a local maximum value, after which the glass temperature has a decreasing trend. The local maximum temperature happens at the middle length for a single glass type and takes place near the right endpoint for the CPC with two covers. This behavior strongly depends on the flow patterns inside the cavities of solar collectors which are quite different. As an important finding, one can notice the glass temperature decrease in CPC with two covers, such that about 2.5 K decrease in the value of average temperature can be found from Fig. 11 due to the installation of the second glass sheet. This behavior proves well the positive effect of two covers in decreasing the energy loss and improving the thermal performance. This improvement occurs by keeping away the high-temperature zone near the absorber from the upper zone near the top glass cover, from which the heat transfer takes place with the ambient. The absorber surface temperature plotted in Fig. 12 also reveals the same behavior, such that more than 3 K increase in the value of average absorber temperature is seen for the CPC with tow panes of glass. This fact causes higher heat flux across the heated absorber towards the working fluid at the bottom of this element. This improvement can also be seen in Fig. 13, in which the distribution of heat flux along the lower surface of the absorber is drawn for the studied two cases.

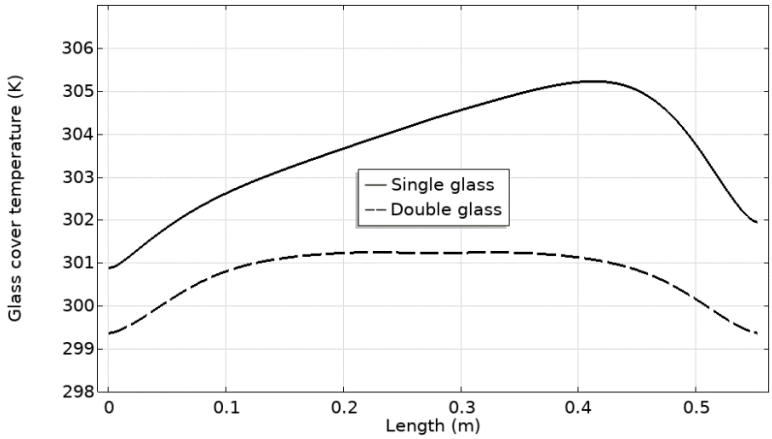

Fig. 11. Glass temperature distribution.

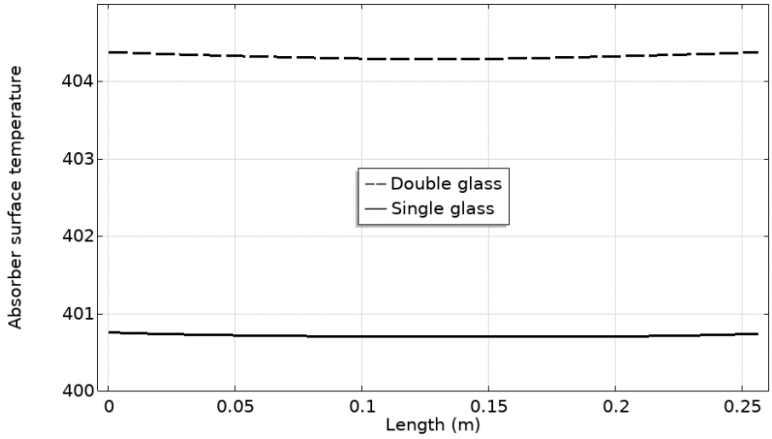

Fig. 12. Temperature distribution along the lower absorber surface.

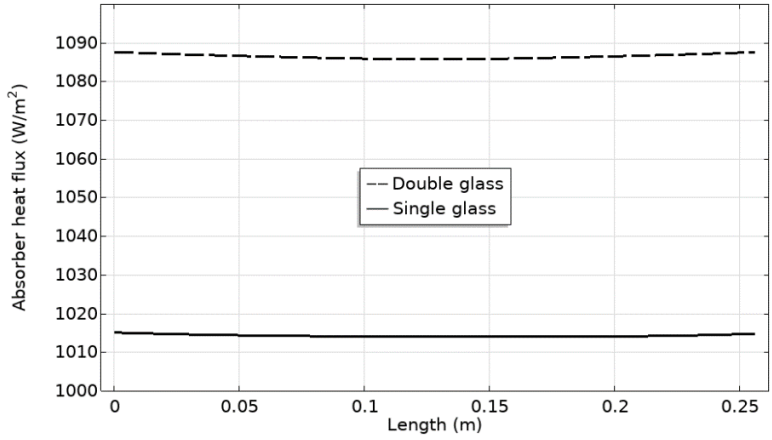

Fig. 13. Heat flux distribution along the lower absorber surface.

The temperature distributions along the vertical centerline of solar collectors which are plotted in Fig. 14 can also show the positive effect of using two covers. The splitting of the high temperature and low-temperature zones by the second glass sheet can easily be seen from this figure. Also, higher absorber temperature and lower glass cover temperature can be distinguished in Fig. 14.

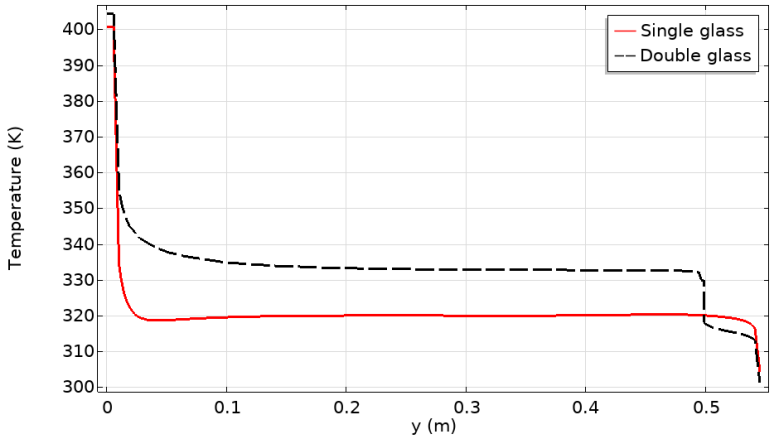

Fig. 14. Temperature distribution along the vertical mid-line.

In order to evaluate the positive effect of installing second glass sheet in CPC, the thermal efficiency which is defined to measure the ability of collector in converting solar incoming radiation into useful energy is computed by the following relation:

$$\eta = \frac{\text{Thermal energy transferred to the working fluid}}{q''_{sun}.A} \tag{6}$$

In Fig. 15, the thermal efficiency of CPC is quantitatively presented as a function of working fluid temperature. For comparison, both single and double glass CPCs are included in the simulation. This figure depicts a decreasing trend for thermal efficiency as the working fluid temperature increases. The effective role of the second glass sheet on performance improvement of double-glazed CPC can be seen in Fig. 15, such that more than 6% as the percentage of efficiency increase can be computed from the curves plotted in this figure.

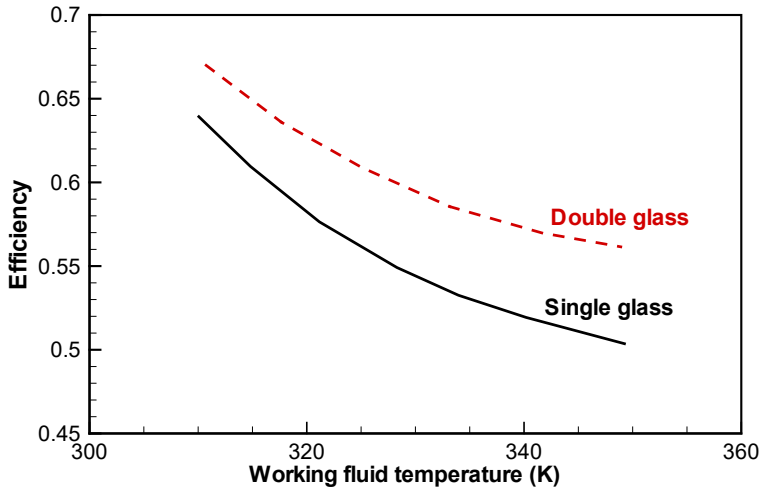

Fig. 15. Variation of CPC efficiency with the working fluid temperature.

4. Conclusion

A 2-D model of CPC solar collectors with two panes of glass was numerically analyzed by the COMSOL Multi-physics 5.5 software in this paper. The role of the second glass sheet under the top glass cover on the thermo-hydrodynamic characteristics of the solar system was examined using the CFD method. The conservation equations for the free convection airflow and conduction equation for computation of temperature distributions in the solid elements were numerically solved, while the well-known $\kappa - \varepsilon$ turbulence model was employed in computations of turbulent stress and heat flux. After extracting the graphical results, the cellular flow pattern due to the presence of free convection flow caused by density gradient and buoyancy-driven flow was quite evident inside the cavity of the collector. For the studied test cases, it was seen that the unicellular recirculated airflow inside the cavity of single glass CPC breaks to the bicellular pattern by installing the second glass sheet, and a more than 6% increase in thermal efficiency was seen due to this technique.

Nomenclature:

A	Area (m^2)	p	Pressure (Pa)
C_R	Concentration ratio	(x, y)	Coordinates system (m)
g	Gravitational acceleration ($m.s^{-2}$)	Greek symbols	
Gr	Grashof number	α_{glass}	Glass absorptivity (-)
h	Convection coefficient (W/m^2K)	β	Volumetric thermal expansion (1/K)
H	Height of collector (m)	ρ_{glass}	Glass reflectivity (-)
k	Thermal conductivity ($Wm^{-1}K^{-1}$)	τ_{glass}	Glass transmissivity (-)
L	Length (m)	δ	Thickness (m)
q	Heat flux (W/m^2)	μ	Viscosity (Pa. s)
Ra	Rayleigh number	ρ	Density (kg/m^3)
T	Temperature (K)	ϑ	Kinematic viscosity (m^2/s)
(u, v)	x- and y- velocity components (m/s)	ϵ	Surface radiation emissivity (-)

References

Abdul-Khalik S I, Li H W, Randall K R (1978), Natural convection in compound parabolic concentrators - A finite element solution, *Journal of Heat Transfer*, 100, 199-204

Antonelli M, Francesconi M, Marco P D, Desideri U (2016). Analysis of heat transfer in different CPC solar collectors: a CFD approach, *Applied Thermal Engineering*,101, 479-489.

Ari R (1975). Comparison of solar concentrators. *Solar Energy*, 18, 93-111.

Buttinger F, Beikircher T, Proll M, Scholkopf M (2010). Development of a new flat stationary evacuated CPC collector for process heat applications. *Solar Energy*, 84, 1166–1174.

Bie Y, Lie M, Chen F, Krolczyk G. Li Z (2020). Heat transfer mathematical model for a novel parabolic trough solar collecting system with V-shaped cavity absorber, *Sustainable cities and society,* 52, 101837.

Cheesewright R, King K J, Ziai S (1986), Experimental data for the validation of computer codes for the prediction of two-dimensional buoyant cavity flows. Significant questions in buoyancy affected enclosure or cavity flows, HTD-60*, ASME Winter Annual Meeting,* Anaheim, December 1986, 75

Chew T C, Tay A O, Wijeysundera N E (1989). A numerical study of the natural convection in CPC solar collector cavities with tubular absorbers, *Journal of Heat Transfer, Transactions of ASME*, 111, 15-23

Diaz G, Winston R (2008). Effect of surface radiation on natural convection in parabolic enclosures, *Numerical Heat Transfer, Part A,*53, 891-906.

Eames P C, Norton B (1993). Detailed parametric study of heat transfer in CPC solar energy collector, *Solar Energy*, 50, 321-338.

Gandjlaikhn Nassab S A (2022). Performance enforcement of a parabolic solar collector with a separating transparent glass sheet, IJEE 13, 158-168.

Jiang C, Yu L, Yang L S, Li K, Wang J, Lund P D, Zhang Y (2020). A Review of the compound parabolic concentrator (CPC) with a Tubular Absorber, *Energies,* 13(3), 695-709.

Marco A, Andrea B, Marco F, Roberto L, Luigi M (2014). Analysis of a low concentration solar plant with compound parabolic collectors and a rotary expander for electricity generation. *Applied Energy* 45, 170-179.

Marco A, Andrea B, Marco F, Umberto D, Luigi M (2015). Electrical production of a small size Concentrated Solar Power plant with compound parabolic collectors. *Renewable Energy,* 83, 1110-1118.

Mill D R, Bassett I M, Derrick G H (1986). Relative cost - effectiveness of CPC reflector designs suitable for evacuated absorber tube solar collectors. *Solar Energy* 36, 199–206.

Mill, D R, Monger A, Morrison G L (1994). Comparison of fixed asymmetrical and symmetrical reflectors for evacuated tube solar receivers. *Solar Energy*, 53, 91–104.

Ochieng R M, Onyango F N (2009). The importance and effect of configurational geometry in the design and application of solar collectors and concentrators with reference to compound parabolic concentrators (CPCs) and cones, *IJEEE* 16, 265-289.

Reichl C H, Hengstberger F, Zauner C (2013). Heat transfer mechanisms in a compound parabolic concentrator: comparison of computational fluid dynamics simulations to particle image velocimetry and local temperature measurements, *Solar Energy*, 97, 436-446.

Singh H, Emaes P H (2012). Correlations for natural convective heat exchange in CPC solar collector cavities determined from experimental measurements, *Solar Energy*,86(9), 2443-2457.